

Flipped Capacitor Based Energy Harvester for Triboelectric Nanogenerators

Alejandro R Oliva

Instituto de Inv. en Ing. Eléctrica, UNS-CONICET
Dpto. de Ing. Eléctrica y de Computadoras
Universidad Nacional del Sur
Bahía Blanca, Argentina
Email: aoliva@uns.edu.ar

Oscar Andrés Aymonino

Instituto de Inv. en Ing. Eléctrica, UNS-CONICET
Dpto. de Ing. Eléctrica y de Computadoras
Universidad Nacional del Sur
Bahía Blanca, Argentina
Email: oscar.aymonino@uns.edu.ar

Abstract—A main drawback of triboelectric generators is the large open circuit voltage that they may produce. A capacitor was connected in parallel with the TriboElectric NanoGenerator (TENG) to reduce the voltage down to a desired value and to force the TENG to have a similar model than a piezoelectric generator (PZG), while reducing the effect of the variable capacitance of the TENG. The Synchronized Switch Harvesting on Capacitor (SSHC) method, originally proposed for piezoelectric generators, was adapted for this application. The proposed flipping algorithm determines the switching instants based on the voltage levels of the capacitors, rather than on fixed times, achieving a charge efficiency of 50% with one flipping capacitor; thus, increasing the amount of harvested energy. Simulation results show the feasibility of the proposed energy harvester, showing that in this example 140% more power can be transferred to the load.

Index Terms—energy harvesting, triboelectric nanogenerator, flexible electronics, wearables, power management, low noise.

I. INTRODUCTION

Flexible electronics is a rapidly evolving technology with significant potential applications such as displays, sensors, smart packaging and wearables. Many of these applications have a relatively large area available for the electronics, that can be fabricated with thin film deposition and patterning processes on paper and plastic substrates with low-temperature roll-to-roll manufacturing techniques or even with a knitting process using smart fabrics. The main advantages of this manufacturing approach are its low-cost and relative low complexity of fabrication that may inspire pioneering products [1] [2]. Continuous advances are made in materials and techniques that make possible new and better passive and active flexible components such as capacitors, inductors, transistors, as well as energy storage devices like flexible batteries and graphene ultracapacitors [3] [4].

The energy to power these circuits is commonly harvested from the surroundings, using photovoltaic (PV) cells, wireless receivers, optical rectennas, thermoelectric and piezoelectric generators [4] [5]. According to [6], as of 2016 PV seemed to be the most suitable energy source to charge *high capacity batteries* from harvested energy because of its relatively

high power density (tens of mW/cm^2), compared to tens to hundreds of $\mu W/cm^2$ for thermal and vibrational sources.

However, this appears to be changing; since in 2012 Wang et al. presented a triboelectric nanogenerator based on the coupling between triboelectric effect and electrostatic induction, which can efficiently convert mechanical energies into electricity [7]. The TENG has many potential advantages, such as large output power, low cost, simple production and high conversion efficiency. For example, there are reports of TENGs, where the area power density can reach up to $50 mW/cm^2$ with a total conversion efficiency close to 85% [8], [9]. Researchers in the Physics area are currently working in this topic; a new and more precise model has been recently introduced by Ghaffarinejad et al., which studies the dynamic behaviours of triboelectric charge generation and build-up [10]. However, a simplified model that considers only static charges will be sufficient to demonstrate the operation of the proposed harvester in this article [11].

The simplest triboelectric generator looks like a capacitor with variable distance between the plates and has a dielectric layer (made of materials A and B) on at least one of its electrodes, as shown in Fig. 1. When the two materials are in contact, opposite static charges, Q , appear on the surfaces due to contact electrification. When the materials separate, a potential difference is created as the materials move apart, modeled by $V_{oc}(x)$ that represents the open circuit voltage; then the voltage that appears across the terminals is

$$V_{teng} = -\frac{Q}{C_{teng}(x)} + V_{oc}(x), \quad (1)$$

where $C_{teng}(x)$ is the distance-dependent capacitance. The output voltage also depends on the materials employed in the fabrication, and could result in high voltages, depending on the test conditions [12].

When an external force modifies the distance between the two materials, the electric variables can be used to sense the applied force or the mechanical energy can be converted into

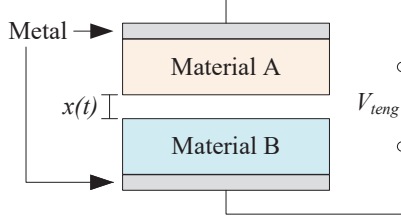


Figure 1. Basic parallel plate TENG.

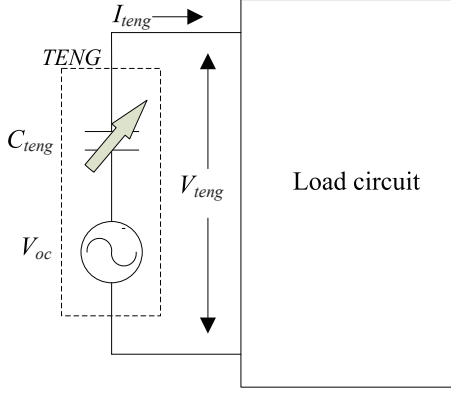


Figure 2. Equivalent circuit of the TENG.

electrical energy. Other types of TENG can transform bending, turning or sliding motion into electricity [13].

A. Electrical characteristics of the TENG

If a circuit is closed between the two metal electrodes an alternating pulsating current with no dc component will flow, according to

$$I_{teng} = C_{teng} \frac{\partial V_{C_{teng}}}{\partial t} + V_{C_{teng}} \frac{\partial C_{teng}}{\partial t}. \quad (2)$$

An equivalent circuit model of the TENG that predicts this behavior is shown in Fig. 2. It comprises a capacitor in series with an ac voltage source, since the inherent capacitance of the TENG blocks any dc current component. Both the capacitance and the voltage depend on the separation between materials A and B, x , which in turn changes in time according to the variations of the external force. Thus, C_{teng} and V_{oc} are time-dependent magnitudes and their rate of change depends on the magnitude and frequency of the external force.

For example, using the same parameters of the experimental TENG analyzed in [14] and reproduced in Table I, the open-circuit voltage varies from 0 to over 33 kV and the capacitance varies from about 3.4 pF to 86 pF for a peak-to-peak displacement of 1 mm. This example exposes an inherent drawback of the TENG due to the large open circuit voltage that it may produce.

According to the equivalent circuit model of the TENG, its output impedance, Z_{teng} , is mainly capacitive and for the

Table I
EXPERIMENTAL TENG PARAMETERS

Variable	Value	Definition
A	$4 \cdot 10^{-4} m^2$	area
ϵ_0	$8.854 \cdot 10^{-12} F/m$	dielectric constant of air
ϵ_{rA}	2.1	dielectric constant of A
ϵ_{rB}	10	dielectric constant of B
d_A	$80 \cdot 10^{-6} m$	width of material A
d_B	$30 \cdot 10^{-6} m$	width of material B
σ	$300 \cdot 10^{-6} C/m^2$	charge density

low frequencies that are normally associated with mechanical forces it may become quite high. The TENG's output impedance is also variable in time and dependent on the applied external force that modifies the distance between the plates. Increasing the velocity of motion is equivalent to increasing the frequency of the ac voltage source V_{oc} ; thus, lowering the output impedance. When the TENG is loaded, the voltage across its terminals, V_{teng} , depends on the voltage divider formed by the internal impedance and the load. It was reported that for a TENG loaded with a variable resistor, the output power presented a maximum for load resistances in the order of the 1-100th of $M\Omega$ and that the current may even show asymmetrical peaks [13].

As of today, most of the literature found around TENG studies the physics, materials and modeling of the TENG, while just a few articles deal with energy harvesters [15]. The objective of this article is to describe an energy harvester suitable for a TENG, by adapting the SSHC technique [16] previously introduced for PZG to the TENG. Section II presents the analysis of the piezoelectric generator with the objective of finding similarities with the triboelectric generator that would be useful in the design of the energy harvester for the TENG. Section III presents the analysis and design considerations of an energy harvester for the TENG based on the conclusions drawn from Section II. Later, in Section IV simulation results are used to analyse and validate the proposed energy harvester. The conclusions to this work are presented in Section V.

II. SYNCHRONOUS SWITCH HARVESTING ON CAPACITORS (SSHC) FOR PIEZOELECTRIC GENERATORS

In contrast with the TENG, the PZG behaves as an ac current source in parallel with a capacitor. The ac current with variable amplitude and frequency that the PZG generates has to be converted into dc voltage by means of a rectifier circuit. The rectifier is able to pass charges from the ac side to the dc side as long as the voltage at the ac side is large enough to forward bias the rectifier. In case of the full-bridge diode rectifier shown in Fig.3, the instantaneous ac voltage has to be larger than $V_1 = V_o + 2V_d$ (where V_o is the dc output voltage and V_d is the forward voltage drop on each rectifier diode). Once the ac voltage drops below this value

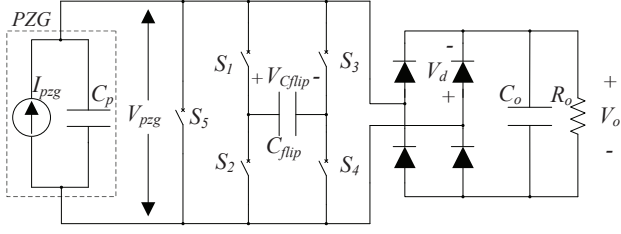


Figure 3. Piezoelectric energy harvester with flipping capacitor.

the capacitor needs to invert its voltage polarity to forward bias the other path of the rectifier bridge, using generated charges to cancel out the stored charges and revert the polarity. Generated charges are wasted in this process, degrading the efficiency of the energy harvesting system. Many techniques have been proposed to improve the charge transfer; among them, the *Synchronized switch harvesting on inductor* (SSHI) rectifier (or inductor-based bias-flip), which is one of the most energy-efficient circuits with ideally no-charge waste [17] [18]. The idea is to synchronously flip the voltage across the PZG to minimize energy waste due to charging and discharging the internal capacitor by means of an auxiliary switched inductor. However, most of the reported implementations require large inductors. An alternative SSH on capacitors (SSHC) approach synchronously flips the voltage across the PZG using one or multiple switched capacitors instead of an inductor, as shown in Fig. 3. The lack of inductors significantly reduces the required system volume [16]. The auxiliary switched capacitor, C_{flip} , is connected in parallel with the PZG (with positive or negative polarity), or left floating. It stores charges that are used to accelerate the voltage flipping process of the internal PZG capacitor, increasing the amount of electrically converted energy during a mechanical loading cycle of the piezoelectric element [16]. When the voltage at the ac side drops below V_1 and no more generated charges are transferred to the dc side, the flipping capacitor, C_{flip} , is connected in parallel with the PZG, then charges are transferred from the internal capacitor, C_p , to C_{flip} until the equilibrium voltage is achieved. C_{flip} is then floated while C_p is short-circuited until its voltage drops down to zero. The next step is to reconnect C_{flip} in parallel with C_p , but with opposite polarity, to aid with the voltage flipping process using the stored charges. Finally, C_{flip} is again floated while C_p is charged from the source until it reaches the voltage that would forward bias the rectifier, i.e., $-V_1$.

In [16] it is shown that if $C_{flip} = C_p$ the optimal voltage flip efficiency for the SSHC interface circuit with one switching capacitor is $\frac{1}{3}$. To understand this, consider the equivalent circuits for the stages of the flipping process shown in Fig. 4, where the arrows indicate the direction in which the charges flow and the labels close to the arrows represent the amount of charges being transferred as a fraction of CV_1 , while the initial charge is indicated close to each capacitor as a fraction of CV_1 . In the steady state and previous to the flipping $V_{C_p} = V_1$

and $V_{C_{flip}} = \frac{1}{3}V_1$, when the two capacitors are connected in parallel they reach a final voltage $V_2 = \frac{2}{3}V_1$. Later on, C_p is completely discharged by means of an auxiliary switch and finally connected in parallel with C_{flip} , but with inverse polarity, until a new equilibrium voltage V_3 is achieved; such that $V_3 = \frac{1}{2}V_2 = \frac{1}{3}V_1$. The total initial charge is $Q_{ti} = \frac{4}{3}CV_1$, while the total final charge is $Q_{tf} = \frac{2}{3}CV_1$. Then the charge efficiency is $\frac{Q_{tf}}{Q_{ti}} = \frac{1}{2}$; meaning that 50 % of the initial charge is still available after the inversion of the voltage of capacitor C_p . This charge would otherwise be wasted in the voltage inversion if the flipping capacitor had not been used. [16] also shows that if 8 auxiliary capacitors were used in the flipping process, the switching efficiency may approach 80 %. In what follows the SSHC concept with one auxiliary capacitor will be applied to a TENG.

III. SYNCHRONOUS SWITCH HARVESTING ON CAPACITOR FOR A TENG

As it was mentioned, the open circuit voltage of a TENG, $V_{oc}(t)$, may reach very high amplitudes that could damage the circuit being powered by the TENG. For example, using the parameters for the TENG summarized in Table 1 of [14] results in an open circuit voltage of $34 kV_{pk}$ for a separation between plates of 1 mm. According to (1) the output voltage could be limited by restricting the displacement of the plates; however, this would also reduce the output power. Another way of reducing the voltage across the TENG is to connect a zener clamp or a bleeding resistor at the output; however this dissipative option degrades the efficiency. A better and more efficient way is to connect an external capacitor in parallel, forming a capacitive voltage divider with the internal capacitor, such that the voltage is now reduced to

$$V_{teng} = V_{oc} \frac{1}{\frac{C_1}{C_{teng}} + 1}. \quad (3)$$

If $C_1 > C_{teng}$ the voltage can be lowered to safe values. For example, if $C_{teng} = 20 pf$, as in Table I, and $C_1 = 10 nf$, yields $V_{teng} = 67.9 V_{pk}$. Furthermore, since $Z_{teng} \gg Z_1$, the TENG behaves as a current source for capacitor C_1 , with magnitude $I_{teng} = \frac{V_{oc}}{Z_{teng}}$. Therefore, the TENG- C_1 combination can be modeled as a current source in parallel with a capacitor, just as the PZG model previously discussed.

A. Analysis for the uncompensated harvester

The uncompensated harvester comprises of the TENG- C_1 combination connected at the ac port of the full-bridge rectifier shown at the left of Fig. 5, with a filter capacitor, C_o and a load resistor R_o connected at the dc port of the bridge.

By analyzing the dc behavior of the circuit, one can realize that the dc current flowing into the rectifier bridge equals the dc output current I_o , since the average current in C_o is zero. Then, considering a sinusoidal generator, the load current is $I_o = \frac{2I_{pk}}{\pi}$ and the dc output voltage is $V_o = I_o R_o$, where I_{pk} is the amplitude of the equivalent current source. Now consider the positive semicycle of the TENG generated current, represented by the blue trace in Fig. 6. As long as the

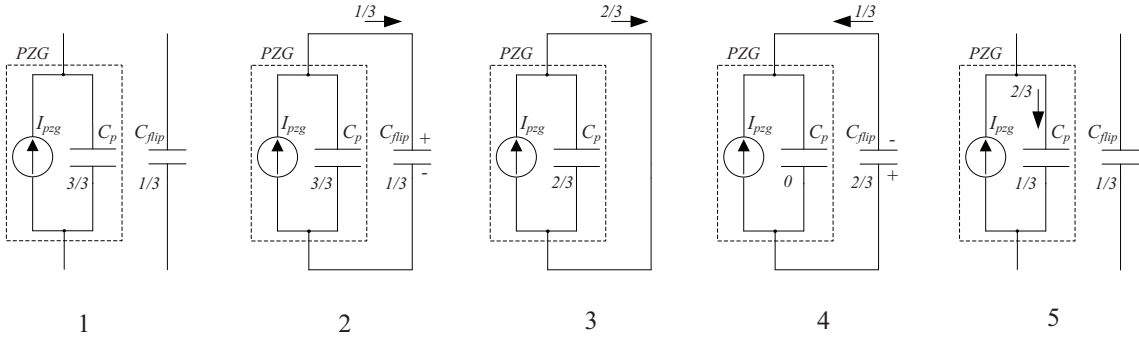


Figure 4. Equivalent circuits for the voltage flipping process of the SSHC for PZG.

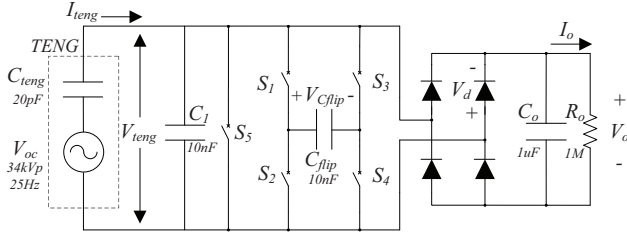


Figure 5. SSHC for TENG.

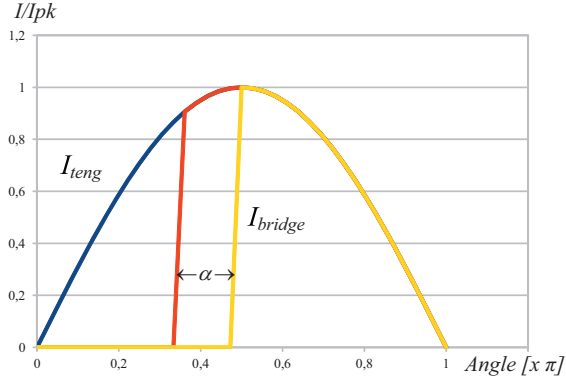


Figure 6. Input current waveform to the bridge rectifier during a half cycle.

voltage at the input of the bridge is larger than $V_1 = V_o + 2V_d$, all the source current flows into the bridge and the voltage of capacitor C_1 is clamped to V_1 . When the source current crosses zero the voltage at the bridge input reaches its maximum value. The current then goes negative, while the capacitor still holds a positive voltage; thus the bridge turns off and the TENG current commutes to C_1 . For the bridge to pass negative current, the voltage across C_1 needs to invert its polarity and reach $-V_1$. At this point the current flows through the bridge and the capacitor voltage gets clamped until the next zero crossing. It is evident that the conduction angle is $\frac{\pi}{2}$ (yellow trace) and that only 50 % of the generated charges pass to the dc side each cycle. For our example, when $I_{pk} = 1.067 \cdot 10^{-4}$ A and $R_o = 1$ M Ω , then $V_o = 33.9$ V.

B. Analysis of the proposed SSHC harvester for TENGs

The circuit in between the TENG- C_1 combination and the diode bridge in Fig. 5 represents the auxiliary system used to compensate the energy harvester. The flipping capacitor, C_{flip} , is connected to a bridge made with four switches ($S_1 - S_4$), that is connected in parallel with the TENG. When switches S_1 and S_4 are active $V_{C_{flip}} = V_{teng}$, otherwise if switches S_2 and S_3 are active $V_{C_{flip}} = -V_{teng}$. When either pair of switches is active C_{flip} is paralleled with C_1 and charges are interchanged between them. Switch S_5 is used to short-circuit C_1 . When all the switches are inactive C_{flip} is floating.

The objective of the improvement in this energy harvester is to increase the conduction in an angle α (such as in the orange trace of Fig. 6) in order to increase the average current and thus the charges that pass to the dc side. If the conduction angle is shifted from $\frac{\pi}{2}$ to $(\frac{\pi}{2} - \alpha)$, then the average current is incremented in $\frac{I_{pk}}{\pi} \sin(\alpha)$ and the average current becomes $I_o = \frac{I_{pk}}{\pi} (1 + \sin(\alpha))$. In the case of using one flipping capacitor with the same capacitance as the one connected at the output of the TENG, that is $C_{flip} = C_1$ and considering $\alpha = 0.47$ rad, the output current increases now to $I_o = 0.49082 \cdot 10^{-4}$ A and $V_o = 49.082$ V. It is evident that more energy has been harvested and reached the load. To determine the maximum value of α it is important to understand the flow of charges during the voltage flipping process. Consider that at $t = 0$ C_1 is charged to V_1 and C_{flip} is charged to $\frac{1}{3}V_1$. Table II summarizes the charge of each capacitor at the end of each stage of the flipping process, while Fig. 7 shows the equivalent circuits for each stage of the process and the initial charge at the beginning of each stage is identified as a fraction of CV_1 .

The charge that C_1 receives in stage 4 from the source to rise the voltage to V_1 is $Q = \frac{2}{3}CV_1$. This charge can be calculated as the time integral of the source current from 0 to $(\frac{\pi}{2} - \alpha)$, as

$$Q = \int_0^{\frac{\pi}{2} - \alpha} \frac{I_{pk}}{\omega} \sin(\omega t) d(\omega t) > \frac{2}{3}CV_1. \quad (4)$$

This limits the maximum angle α to

$$\alpha_{max} = \arcsin \left(1 - \frac{2}{3}CV_1 \frac{\omega}{I_{pk}} \right), \quad (5)$$

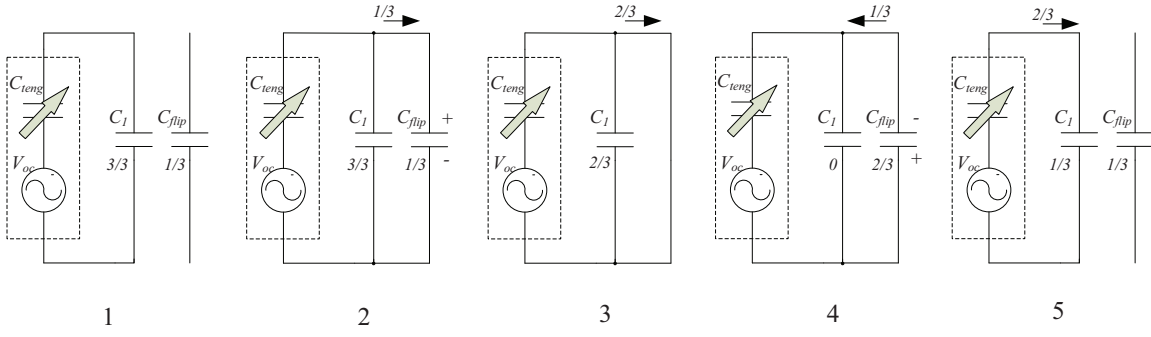


Figure 7. Equivalent circuits for the voltage flipping process of the SSHC for TENG.

Table II
CHARGE FLOW DURING THE FLIPPING PROCESS

stage	charge C_1	flow direction	charge C_{flip}
$t=0$	$\frac{3}{3}CV_1$	-	$\frac{1}{3}CV_1$
1	$\frac{2}{3}CV_1$	$\frac{1}{3} \text{ --- } >$	$\frac{2}{3}CV_1$
2	0 shorted	-	$\frac{2}{3}CV_1$ no change
3	$\frac{1}{3}CV_1$	$< \text{ --- } \frac{1}{3}$	$\frac{1}{3}CV_1$
4	$\frac{3}{3}CV_1$	$\frac{2}{3}$ from source	$\frac{1}{3}CV_1$ no change

where $V_1 = f(\alpha)$. With a larger angle the source would not have enough charges to complete the flipping process, and with a smaller angle charges that could otherwise pass to the dc side would be wasted. The angle found here is not only the maximum but the optimal one. This shows that the timing is crucial and that it is more efficient to produce the switching at the right voltage level rather than at fixed time instants.

In [16] once the instant to start flipping the capacitor voltage is detected, the described flipping sequence commences, using fixed time intervals for each step generated by a digital circuit. In this work the starting time of the flipping sequence is detected as in [16], coincident with the zero crossing of the current, and thus it commences synchronously with the dropping below V_1 ; however, in contrast, the duration of each flipping stage is determined asynchronously, based on the voltage levels that indicate the adequate charge of the capacitors (those from Table II).

IV. SIMULATION RESULTS AND DESIGN CONSIDERATIONS

The schematic circuit of the energy harvester shown in Fig. 5 was implemented in LTspice® considering losses in the switches and diodes; capacitors and sources were considered lossless. The switches were modeled as an ideal switch, SW, using $R_{on} = .1\Omega$ and $R_{off} = 1000M\Omega$, while the diodes were modeled using the built in 1N4148 model.

Fig. 8 shows the current and voltage waveforms for the uncompensated (blue) and the compensated (red) energy harvesters. The top waveforms correspond to the current flowing into the bridge rectifier, while the bottom waveforms corre-

spond to the voltage across the input of the bridge that is equal to V_{teng} . The current waveforms show a spike near the zero crossing, where the flipping process takes place, mostly because the short circuit of C_1 also shorts the TENG. If necessary, short-circuiting the TENG could be avoided by adding an extra switch in series with it. The conduction starts at $\frac{\pi}{2}$ for the uncompensated harvester, while the conduction angle has been extended for the compensated harvester. The voltage waveforms show that the voltage flipping time has been considerably shortened and the peak voltage has increased by using the compensator. In consequence, the average output voltage changes from 31.26 V for the uncompensated up to 48.49 V for the compensated harvester. This improvement translates into 140.6% more power being transferred to the load.

V. CONCLUSION

When a TENG is loaded with a parallel capacitor its output voltage can be reduced and its equivalent circuits mimics that of a PZG. Then it is feasible to adapt a SSHC to use with a TENG while achieving a good charge efficiency. In this case, using only one flipping capacitor the power transferred to the load was incremented by 140%. Only the conduction losses in switches and diodes were taken into consideration; the figure will decrease when considering the gating and switching losses. It is possible that by using more switching capacitors, in such a way that the charge transfer between the capacitors occur at similar voltage levels, the efficiency could be increased. A trade off should be made in this case between the gain and the increased losses introduced by the new switches. To increment the amount of harvested energy is better to reduce the parallel capacitance; but, this capacitance is needed to reduce the voltage of the TENG. Alternatively, operating the TENG with a lower open circuit voltage would require a smaller flipping capacitor, so the charges required to flip its voltage would be reduced; however, the power produced by the TENG would be also smaller.

ACKNOWLEDGMENT

The authors would like to thank Universidad Nacional del sur, CONICET and FONCyT for their financial support.

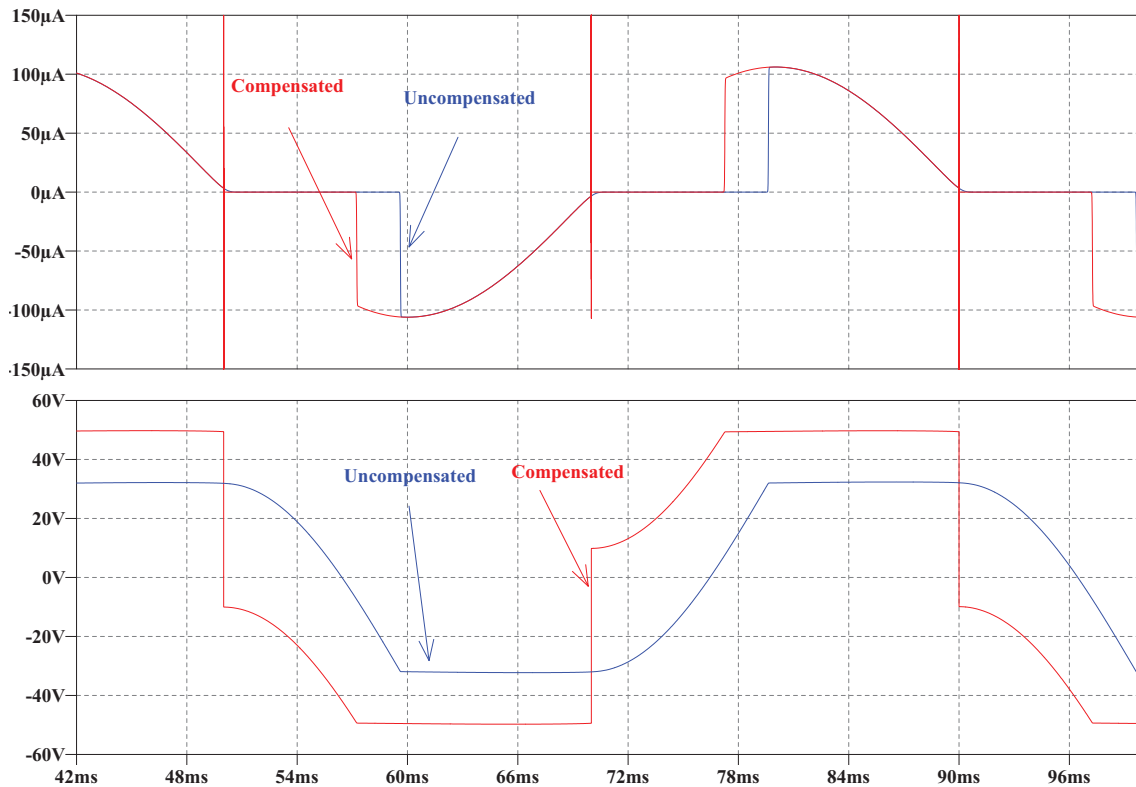


Figure 8. Current and voltage waveforms for the uncompensated and compensated energy harvesters. Top figure: current flowing into the bridge rectifier, bottom figure: voltage across the TENG.

REFERENCES

- [1] R. D. Bringans and J. Veres, "Challenges and opportunities in flexible electronics," in *2016 IEEE International Electron Devices Meeting (IEDM)*, Dec 2016, pp. 6.4.1–6.4.2.
- [2] E. W. Forsythe, B. Leever, M. Gordon, R. Vaia, D. Morton, M. Durstock, and R. Woods, "Flexible electronics for flexible and defense applications," in *2015 IEEE International Electron Devices Meeting (IEDM)*, Dec 2015, pp. 19.1.1–19.1.4.
- [3] M. F. El-Kady and R. B. Kaner, "Scalable fabrication of high-power graphene micro-supercapacitors for flexible and on-chip energy storage," *Nature Communications*, vol. 4:1475, 2013.
- [4] A. Nathan, A. Ahnood, M. T. Cole, S. Lee, Y. Suzuki, P. Hiralal, F. Bonaccorso, T. Hasan, L. Garcia-Gancedo, A. Dyadyusha, S. Haque, P. Andrew, S. Hofmann, J. Moultrie, D. Chu, A. J. Flewitt, A. C. Ferrari, M. J. Kelly, J. Robertson, G. A. J. Amaratunga, and W. I. Milne, "Flexible electronics: The next ubiquitous platform," *Proceedings of the IEEE*, vol. 100, no. Special Centennial Issue, pp. 1486–1517, May 2012.
- [5] A. E. Ostfeld, A. Gaikwad, Y. Khan, and A. Arias, "High-performance flexible energy storage and harvesting system for wearable electronics," *Scientific Reports*, vol. 6, 05 2016.
- [6] A. Erin Ostfeld and A. Arias, "Flexible photovoltaic power systems: Integration opportunities, challenges and advances," *Flexible and Printed Electronics*, vol. 2, 01 2017.
- [7] F. Fan, Z.-Q. Tian, and Z. Wang, "Flexible triboelectric generator," *Nano Energy*, vol. 1, p. 328?334, 03 2012.
- [8] G. Zhu, Y. Sheng Zhou, P. Bai, X. Song Meng, Q. Jing, J. Chen, and Z. Wang, "A shape-adaptive thin-film-based approach for 50% high-efficiency energy generation through micro-grating sliding electrification," *Advanced materials (Deerfield Beach, Fla.)*, vol. 26, 06 2014.
- [9] Y. Xie, S. Wang, S. Niu, L. Lin, Q. Jing, J. Yang, Z. Wu, and Z. Wang, "Grating-structured freestanding triboelectric-layer nanogenerator for harvesting mechanical energy at 85% total conversion efficiency," *Advanced materials (Deerfield Beach, Fla.)*, vol. 26, 10 2014.
- [10] A. Ghaffarinejad and J. Yavand Hasani, "Modeling of triboelectric charge accumulation dynamics at the metal-insulator interface for variable capacitive structures: application to triboelectric nanogenerators," *Applied Physics A*, vol. 125, 04 2019.
- [11] S.-H. Shin, Y. Eun Bae, H. Kyung Moon, J. Kim, S.-H. Choi, Y. Kim, H. Jae Yoon, M. H. Lee, and J. Nah, "Formation of triboelectric series via atomic level surface functionalization for triboelectric energy harvesting," *ACS Nano*, vol. 11, 05 2017.
- [12] B. W. Lee and D. E. Orr, "The triboelectric series," <https://www.alphalabinc.com/triboelectric-series>, 2009.
- [13] S. Niu, Y. Sheng Zhou, S. Wang, Y. Liu, L. Lin, Y. Bando, and Z. Wang, "Simulation method for optimizing the performance of an integrated triboelectric nanogenerator energy harvesting system," *Nano Energy*, vol. 8, 09 2014.
- [14] B. Yoon, J. M. Baik, and K. A. Kim, "Circuit modeling approach for analyzing triboelectric nanogenerators for energy harvesting," in *2018 International Power Electronics Conference (IPEC-Niigata 2018 -ECCE Asia)*, May 2018, pp. 3063–3068.
- [15] I. Park, J. Maeng, D. Lim, M. Shim, J. Jeong, and C. Kim, "A 4.5-to-16uW integrated triboelectric energy-harvesting system based on high-voltage dual-input buck converter with mppt and 70V maximum input voltage," in *2018 IEEE International Solid - State Circuits Conference - (ISSCC)*, Feb 2018, pp. 146–148.
- [16] S. Du and A. A. Seshia, "An inductorless bias-flip rectifier for piezoelectric energy harvesting," *IEEE Journal of Solid-State Circuits*, vol. 52, no. 10, pp. 2746–2757, Oct 2017.
- [17] A. Badel, D. Guyomar, E. Lefeuvre, and C. Richard, "Efficiency enhancement of a piezoelectric energy harvesting device in pulsed operation by synchronous charge inversion," *Journal of intelligent material systems and structures*, vol. 16, pp. 889–901, 10 2005.
- [18] Y. Ammar and S. Basrour, "Circuit modeling approach for analyzing triboelectric nanogenerators for energy harvesting," in *Design, Test, Integration and Packaging of MEMS / MOEMS (DTIP 2006)*, Stresa, Lago Maggiore, Italy. TIMA Editions, Apr 2006, p. 5.